Journal Name

ARTICLE

Supporting Information

DNA-Templated Silver Nanoclusters: Structural Correlation and Fluorescence Modulation

S. Y. New,[*a] S. T. Lee[a] and X. D. Su[*b]

[a] School of Pharmacy, Faculty of Science, University of Nottingham Malaysia Campus, Jalan Broga, 43500 Semenyih, Selangor Darul Ehsan, Malaysia. Email: SiuYee.New@nottingham.edu.my; Tel: +603 8924 8762
[b] Institute of Materials Research and Engineering, 3 Research Link, Singapore 117602. E-mail: xd-su@imre.a-star.edu.sg; Tel: +65 6874 7091

Journal Name

ARTICLE

Table S1. Reported primary structure ssDNA used to form AgNCs

	DNA sequence (5'→3')	$\lambda_{ex}/\lambda_{em}$ (nm)	N_{Ag}	Quantum Yield (%)	Synthesis ratio (DNA:Ag^+:BH_4^-)	Buffer	Remarks	Ref
First reported DNA-AgNCs	1) $AG_2TCGC_2GC_3$	540–580/629–642	1–4	N/A	1:6:6	5 mM PBS pH 7.5 or 100 mM $NaClO_4$ or 5 mM PBS pH 7.5	- N_{Ag} is determined from ESI-MS.	[1]
Homopolymers	2) C_n (n = 5–11)	350–850/500–950	10	N/A	1:11:6.1	10 mM NH_4OAc, pH 6.8	- N_{Ag} is determined from ESI-MS. - Homo-A, homo-T and series of mixed A/T strands yield no fluorescence at neutral pH. - For C_n runs, n should be >4. - For G_n runs, n should be >5. - Terminal T in (3) is to increase synthesis yield and enhance analysis for ESI-MS.	[2]
	3) TG_nT (n = 3–6, 8, 9, 11)	350–850/500–950						
	4) A_n (n = 6, 9, 11)	No fluorescence						
	5) T_n (n = 6, 9, 11)	No fluorescence						
	6) Series of mixed A/T strands	No fluorescence						
Cytosine- and thymine-rich DNA	7) C_{12}	340/485; 440/525; 280 or 580/665; 650/700	5; 4; 3; 2	1; N/A; 23; 17	1:6:6	5 mM acetate buffer or PBS	- N_{Ag} is determined from Job's plot of emission intensity *vs.* [DNA]:[Ag^+]. - Thymine-rich DNAs favour blue/green emitters; whereas cytosine-rich DNAs prefer red emitters. - (7)-AgNCs form multiple species: blue and green emitters (λ_{em} = 485 and 525 nm) are partially oxidised species and	[3–6]
	8) T_{12}	350/545	6	14		5–10 mM borate buffer, pH 10.5		
	9) $T_4C_4T_4$	370/475	6	N/A				
	10) $C_4T_4C_4$	340/495 or 580/650	8	N/A				

	DNA sequence (5'→3')	$\lambda_{ex}/\lambda_{em}$ (nm)	N_{Ag}	Quantum Yield (%)	Synthesis ratio (DNA:Ag^+:BH_4^-)	Buffer	Remarks	Ref
							interconvertible with fully reduced red emitters (λ_{em} = 665 nm). - (7)-AgNCs in PBS buffer preferentially stabilises NIR species (λ_{em} = 700 nm). - Basic pH is needed to deprotonate N3 of thymine (pKa = 9.7) for clusters-binding. - (8)- and (9)-AgNCs are partially oxidised species. - Low concentration of (10) favours blue/green species; whereas high concentration favours red-emitters; attributed to intramolecular *vs.* intermolecular cluster templates.	
	11) (C**X**G)n, X = A, T, C or G; n = 6–9	512/600 (X = G/C; n = 6)	N/A	N/A	1:8:16	20 mM PBS, pH7.0 with 1 mM $Mg(OAc)_2$	- By varying synthesis ratio, type of middle base (X) or number of trinucleotide repeats (n), only emission intensity is affected. - X = G gives the highest emission intensity, followed by C. - No fluorescence observed when X = A/T.	7
Effect of C–Ag^+–C pairs 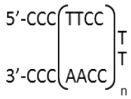	12) n = 1	460/536	2	8	1:6:6	20 mM PBS, pH 7.0	- N_{Ag} is determined from ESI-MS. - C_3 at 5' and 3'-ends helps to stabilise AgNCs. - Higher number of A–T pairs in repeating units (n) may hinder the coordination of C–Ag^+–C. - Higher number of repeated CC bases results in larger AgNCs.	8
	13) n = 2	540/608	4–5	61				
	14) n = 5	540/620	5–6	21				
	15) n = 6	540/644	6	25				

	DNA sequence (5'→3')	$\lambda_{ex}/\lambda_{em}$ (nm)	N_{Ag}	Quantum Yield (%)	Synthesis ratio (DNA:Ag^+:BH_4^-)	Buffer	Remarks	Ref
Chemopalette-1[a]	16) $C_3T_3A_2C_4$ (B)	340/485	N/A	N/A	1:6:6	Water	- Longer λ emitters show better photo- and chemical stability in buffer. - Preparation under crowded crowding condition (*i.e.* in presence of PEG 200) has improved the quantum yield.	9,10
	17) $C_3TCT_2A_2C_3$ (G)	425/520		16 ± 3		Water		
	18) $C_3T_2A_2TC_4$ (Y)	475/572[c]; 475/560[d, e]		38 ± 2[c]; 6.4[d]; 66.2[e]		20 mM PBS, pH 6.5–8[c]; 25 mM PBS, pH 7.0[d]; 25 mM PBS with 30% PEG 200[e]		
	19) $A_2T_2C_{12}A_2T_2$	N/A (Yellow)		68		N/A		
	20) $C_2TC_2T_2C_2TC_2$ (R)	543/620[c]; 580/616[d,e]		32 ± 4; 24.5[c]; 67.6[d]		20 mM citrate, pH 5[c]; 25 mM PBS, pH 7.0[d]; 25 mM PBS with 30% PEG 200[e]		
	21) $C_3TA_2CTC_4$ (N)	650/705		34 ± 5		20 mM NH_4OAc, pH 6.5–8		
Chemopalette-2	22) $TGACTA_4C_3T_2A_2TC_4$	460/550	20–30	0.2	1:6:6	20 mM PBS, pH 6.6 or water	- N_{Ag} is determined from Ag K-edge EXAFS. - Ag–DNA ligation, cluster size and Ag–Ag bonding cooperatively modulate fluorescence properties of AgNCs.	11,12
	23) $AGTCAC_4A_2C_2TGC_3TAC_2ACG_2ACT$	530/600	8–14	10				
	24) $G_2CAG_2T_2G_4TGACTA_5C_3T_2A_2TC_4$	595/650	8–14	64				
	25) $AGTC_2GTG_2TAG_3CAG_2T_2G_4TGACTA_5C_3T_2A_2TC_4$	640/700	8	52				
Chemopalette-3	26) $(CCCTA_2)_3CCCTA$	468/560	N/A	N/A	1:6:6	10 mM Tris/ HCl, pH 7.0	- Alternation of single C to G (as underlined) in (26) causes blue-shift in emission. - Double and triple C to G mutations accounts for the remarkable red-shift.	13
	27) $(C\underline{G}CTA_2)_3C\underline{G}CTA$	466/554						
	28) $(CC\underline{G}TA_2)_3CC\underline{G}TA$	439/495						
	29) $(\underline{GG}CTA_2)_3\underline{GG}CTA$	453/515						
	30) $(\underline{GCG}TA_2)_3\underline{GCG}TA$	548/623						
	31) $(\underline{GGG}TA_2)_3\underline{GGG}TA$	560/626						
Chemopalette-4	32) $CGC_6T_2G_2CGT$	270/558	21[b]	N/A	1:10:2.4	10–40 mM NH_4OAc buffer, pH 7	- N_{Ag} is determined from HPLC-MS. - Mixed species were purified *via* HPLC-MS. - Only N_{Ag} of bright species is shown. Dark species appear at lower N_{Ag} and are not shown here. - Larger clusters tend to emit at longer λ_{em}.	14–16
	33) CGC_6TCG_2CGT	270/557	21[b]		1:6:3			
	34) $TGC_2T_4G_4ACG_2ATA$	270/562	10		1:12.5:6.27			
	35) $T_2C_4AC_2AC_3AG_2C_4GT_2$	270/632	16		1:12:6			
	36) $T_2CGC_6GC_4AG_2CGT_2$	270/644	15		1:12:6			
	37) $C_3AC_3AC_3TC_3A$	270/777	20[b]		1:8:4			

	DNA sequence (5'→3')	$\lambda_{ex}/\lambda_{em}$ (nm)	N_{Ag}	Quantum Yield (%)	Synthesis ratio ($DNA:Ag^+:BH_4^-$)	Buffer	Remarks	Ref
IR emitting species	38) $C_3AC_3AC_3TC_3A$	750/810	10	30 ± 2	1:8:4	10 mM citrate buffer, pH 7.0	- N_{Ag} is determined from ICP-AES. - Based on general sequence $C_3AC_3AC_3XC_3Y$. - Chromatographically separated and identified with AES study.	15,16
	39) $C_3AC_3AC_3GC_3A$	720/770	9–10	30 ± 5				
	40) $C_3AC_3AC_3AC_3G$	840/870	9	6 ± 2				
AgNCs with enhanced stability	41) $AC_3GA_2C_2TG_3CTA_2A_3T_2A_2T_4$	535/615	N/A	30	1:6:6	20 mM PBS, pH 6.8	- Shelf-life of > 1 year. - Highly resistant to oxidation, pH and temperature.	17
Intergrowth of emitter pair [a] 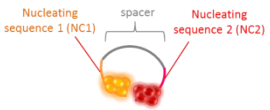	NC1 – X_n – NC2; NC1 and NC2: sequence (16) to (21) from *'Chemopalette-1'*; X = A, T, C or G; n = 0–70	λ_{em} ~604 (YN, NN, BN, RN and GN) λ_{em} ~630 for other combination	N/A	16.3 (for Y – T_{15} – N)	1:6:6	5 mM PBS containing 50 mM $NaNO_3$, pH 7.0	- The optimised base type for spacer (X) is T, which also shows length-dependent fluorescence. The best length (n) is 15. - Disruption of spacer through hybridization with complementary sequence significantly decreases the fluorescence.	18
Chameleon-like violet clusters	42) $C_3AC_3AC_3TC_3AC_3GC_2GCTG_2A$	NA/790	11	N/A	1:8:4	10 mM citrate/citric acid buffer, pH 6.5	- N_{Ag} is determined from stoichiometry study from absorption spectra. - Chromatographically purified. - Underlined sequence denotes the nucleation template, with the following sequence as recognition site. - (42) derives from (38). - (42)- and (43)-AgNCs transform the weakly emissive violet chromophore to strong NIR and green emitter respectively ($\Delta\lambda_{abs}$ 330 & 90 nm). - The changes are due to alteration of shape and structure of DNA host	19,20
	43) $C_4A_2CTC_2T_2C_3GC_2AC$	490/550	11					

	DNA sequence (5'→3')	$\lambda_{ex}/\lambda_{em}$ (nm)	N_{Ag}	Quantum Yield (%)	Synthesis ratio ($DNA:Ag^+:BH_4^-$)	Buffer	Remarks	Ref
							upon binding. - Violet clusters are favoured when Ag^+:DNA = 4–10 and prepared at high oxygen pressure.	
AgNCs with high yield	44) $T_2CC_3AC_3A_4G_2C_3GT_2$	571/635	24[b]	94 ± 8	1:10:10	10 mM NH_4OAc	- AgNCs with the highest quantum yield reported to date.	[21]

[a] Abbreviation of sequences are given in (), with B, G, Y, R, N represent blue, green, yellow, red and NIR emitters respectively.

[b] N_{Ag} for strand dimer complexes.

[c, d, e] $\lambda_{ex}/\lambda_{em}$ (nm) and quantum yield of AgNCs formed at the corresponding buffer.

Please do not adjust margins

Table S2. Reported i-motif and G-quadruplex templates that have been used to form AgNCs

	DNA sequence (5'→3')	$\lambda_{ex}/\lambda_{em}$ (nm)	N_{Ag}	Quantum Yield (%)	Synthesis ratio (DNA:Ag^+:BH_4^-)	Buffer	Remarks	Ref.
i-motif 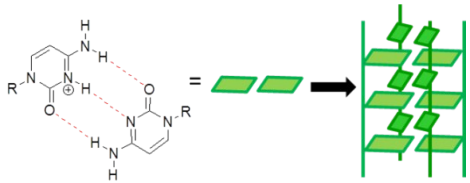	45) $(TA_2C_4)_4$	460/560 560/625	N/A	N/A	1:16:16	10 mM formate/cacodylate/PBS/borate, pH 5–9	- Both (45)- & (46)-AgNCs show pH-dependent optical behaviour. - Red species is dominant at pH 6, which is the optical pH for i-motif. This is further corroborated by SEC. - Green species is most favoured at pH 8–9. SEC study revealed that it is entrapped within similar structure as i-motif.	22
	46) $(C_4A_2)_3C_4$	500/570 560/625						
	47) $C_4A_4C_3$	543/613[a,b]	1–4[b]	16 ± 2[a]; 37 ± 2[b]	1:4:4	MES containing 50 mM Na^+, pH 5[a]; PBS, pH 7[b]; 25 mM PBS, pH7[c]; 25 mM PBS, pH7, 30% PEG 200[d]	- N_{Ag} is determined from HPLC-MS. - (47) & (48): intermolecular i-motif. - (49) & (50): intramolecular i-motif.	10,23
	48) $C_4A_4C_4$	575/635[a,b]; 540/600[c,d]	N/A	11 ± 2[a]; 12 ± 1[b]; 14.5[c]; 32.1[d]	1:4:4			
	49) $(C_3TA_2)_2C_2TA_2C_3T$	463/538[a,b]; 520/575[c,d]	5–8[a]	10 ± 2[a]; 6.7[c]; 34.7[d]	1:6:6			
	50) $GC_5(GC_4)_3T$	582/655[a,b]	N/A	11 ± 1[a]	1:6:6			
	51) $C_4–X_1X_2X_3X_4–C_4$ X = mixture of A/T	570–590/615–630	N/A	78 (X = ATAT)	1:6:1	10 mM PBS, pH 7.6	- Changing the position of T can modulate the quantum yield. - X = ATAT gives the best yield, but changing it to TATA reduces the yield to 15%.	24
G-quadruplex 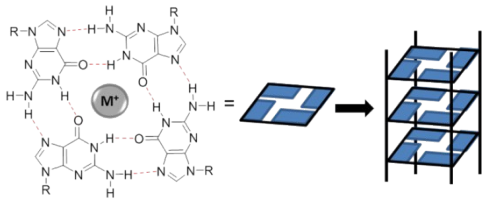	52) $(G_2T)_4T_2G(TG_2)_4$	325/420; 510/680	2	N/A	1:6:6	20 mM PBS containing 10 mM KCl, pH 8	- N_{Ag} is determined from MALDI-TOF MS.	25
	53) $(G_3T_2A)_3G_3$	390/435	1					
	54) $(G_4T_4)_3G_4$	430/565	2					
	55) $G_3TAG_3CG_3T_2G_3$	435/565	2					
	56) $(G_3T)_4$	425/560	2					
	57) $GTG_3TAG_3CG_3T_2G_2$	240/390	3					

	DNA sequence (5'→3')	$\lambda_{ex}/\lambda_{em}$ (nm)	N_{Ag}	Quantum Yield (%)	Synthesis ratio ($DNA:Ag^+:BH_4^-$)	Buffer	Remarks	Ref.
	58) $G_3T_4G_4$	580/652	2–4[a]	10 ± 2[a]	1:4:4	57–60) MES containing 50 mM Na^+, pH 5[a]; PBS, pH 7[b]	- N_{Ag} is determined from ESI-MS. - (58) & (59): intermolecular G-quadruplex. - (60) & (61): intramolecular G-quadruplex.	23
	59) $G_4T_4G_4$	580/648	N/A	8 ± 2[a]	1:4:4			
	60) $AG_3(T_2AG_3)_3$	557/621	5–12[a]	7 ± 2[a]	1:6:6			
	61) $A(G_4C)_3G_5C$	610/670	N/A	10 ± 2[a]	1:6:6			
	62) $(AG_3)(T_2AG_3)_3$	445/520; 560/620	N/A	N/A	1:6:6	Deionised water	- Red emitters are associated with G bases, whereas green emitters are located between A and G bases. - In the presence of Na^+, fluorescence is significantly quenched as a result of anti-parallel G-quadruplex formation.	26
Logic gate using G-quadruplex & i-motif as templates:	63) $G_3T_2AG_3T–C_6–AC_3T_2AC_3$	494/570; 581/646[a] or 537/601[b]	N/A	N/A	1:6:6	10 mM TrisOAc, pH 8[a] or 10 mM TrisOAc containing 100 mM K^+, pH5.0[b]	- (63) and (64) exist as hairpin structures without K^+ and H^+ inputs. - In the presence of K^+ and H^+, G- and C-tracts (shown in red and blue respectively) are convertible to G-quadruplex and i-motif. - (63)-AgNCs shows emission in orange region due to structural change; whereas (64) -AgNCs show different intensity in yellow and red region.	27
	64) $(G_3T)_2–C_6–(AC_3)_2$	512/582; 575/634				10 mM TrisOAc, pH 8		

[a, b] $\lambda_{ex}/\lambda_{ex}$ (nm) and quantum yield of AgNCs formed at the corresponding buffer.

Please do not adjust margins

Table S3. A summary of hairpin loop-hosted AgNCs

	DNA sequence (5'→3')	$\lambda_{ex}/\lambda_{em}$ (nm)	N_{Ag}	Quantum Yield (%)	Synthesis ratio ($DNA:Ag^+:BH_4^-$)	Buffer	Remarks	Ref.
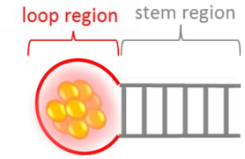							- Loop region is the primary site for nucleation and encapsulation of AgNCs.[28–31] - Loop size should be > 3 bases, otherwise it is sterically impossible to form.[32]	
(i) Loop of different base type:	$TATC_2GT-X_5-ACG_2ATA$			N/A	1:5.6:11.2	40 mM NH_4OAc, pH 6.9	- N_{Ag} is determined from ESI-MS. - (65)- and (66)-AgNCs contain smaller N_{Ag} than the rest, even though they are brighter.	30
	65) X = C	581/643	1					
	66) X = G	544/641	1					
	67) X = T	N/A	2					
	68) X = A	471/534	2 [a]					
(ii) C-loop of different size:	69) $TATC_2GT-C_n-ACG_2ATA$ n = 3–12	**Group I:** 553–600/614–668 (n = 3–8) **Group II:** 543–560/610–628 (n = 9–12) **Group III:** 450–483/534–596 (n = 4–8; 11–12) **Group IV:** 407–413/524–530 (n = 9–10)	N/A	34 (n = 7; red emitter); 3.7 (n = 9; green emitter)	1:6:2	40 mM NH_4OAc, pH6.9	- Grouping (I – IV) is defined by abrupt fluorescence attenuation as loop size (n) increases. - All samples, except n = 3, produce distinct red and green species. - For group I and III, λ_{em} generally red-shifts as loop size increases.	29
	70) CCCCCCC $-C_8-$ GCCCGCC	438/520; 557/626	N/A	N/A	1:18:8	20 mM HEPES, pH7.6		33
	$GCATATCG-C_n-CGATATGC$ 71) n = 5	466/522; 555/649	N/A	N/A	1:18:8	20 mM HEPES, pH7.6	- All samples, except (73) and (74) produce distinct red and green species. - Green emitters are oxidised species, whereas the red one as reduced species. - Light exposure and $NaBH_4$ treatment reversibly decrease and recover fluorescence. Anti-correlation was observed for green emitters.	33
	72) n = 8	450/550; 530/630						
	73) n = 11	564/630						
	74) n = 14	570/635						

	DNA sequence (5'→3')	$\lambda_{ex}/\lambda_{em}$ (nm)	N_{Ag}	Quantum Yield (%)	Synthesis ratio ($DNA:Ag^+:BH_4^-$)	Buffer	Remarks	Ref.
							-Addition of Hg^{2+} weakens the binding of DNA-Ag and causes irreversible quenching.	
(iii) T-loop with C-/G-rich stem:	75) $(ACCC)_3$–T_n– $(GGGT)_4$ n = 0, 4, 5, 6, 8, 10	512/581; 580/639	1–4 (n = 5)	N/A	1:6:6	10 mM Tris-HNO_3, pH7.0	- Red fluorescence (λ_{em} = 639 nm) is 7x weaker than yellow (λ_{em} = 581 nm). - For (75), when n = 0, excited-state lifetime is shorter and fluorescence intensity is 12.5x weaker. - (75) with varied loop size shows innocuous result due to weak binding of Ag^+ to T. - Fluorescence intensity increases as x increases, elucidating that longer stem may provide better protection environment. - Adding Mg^{2+}, Pb^{2+} or K^+ affects the stability of stem duplex or converts G-rich strand to G-quadruplex, thus influencing the emission intensity. This enables logic gate construction.	31
	76) $(AACCC)_x$–T_5– $(GGGT)_x$ x = 1–4		N/A					

Table S4. Reported dsDNA templates that have been used to form AgNCs

	DNA sequence	$\lambda_{ex}/\lambda_{em}$ (nm)	N_{Ag}	Quantum Yield (%)	Synthesis ratio (DNA:Ag^+:BH_4^-)	Buffer	Remarks	Ref.
Duplex 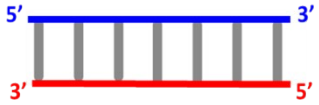	77) 5′-$G_3T_4G_4$-3′ 3′-$C_4A_4C_3$-5′	554/616	2–6	5 ± 1	1:4:4	PBS, pH 7	- N_{Ag} is determined from ESI-MS. - By comparing the duplex with individual C- & G-rich strands, duplex binds more Ag^+.	23
	78) 5′-$G_4T_4G_4$-3′ 3′-$C_4A_4C_4$-5′	635/706	N/A	7 ± 1	1:4:4			
	79) 5′-A(G_4C)$_3G_5C$-3′ 3′-T(C_4G)$_3C_5G$-5′	597/666		10 ± 1	1:6:6			
	80) 5′-(C_3A)$_2C_3$GAGA(TGC)$_2$-3′ 3′-(G_3T)$_2G_3$CTCT(ACG)$_2$-5′	517/583	N/A	N/A	1:10:10	0.02 M PBS, pH 7.4	- Longer C in (82) & (83) stimulates higher fluorescence intensity. - Hybridisation with G-rich strand can enhance the fluorescence. - Longer G-strand (83) stimulates higher fluorescence intensity, as compared to (82).	34
	81) 5′-(C_3A)$_2C_3$ GAGA(TGC)$_2$-3′ 3′-(TG_3)$_4$CTCT(ACG)$_2$-5	515/579						
	82) 5′-(C_3A)$_4$GAGA(TGC)$_2$-3′ 3′-(G_3T)$_2G_3$CTCT(ACG)$_2$-5′	515/577						
	83) 5′-(C_3A)$_4$GAGA(TGC)$_2$-3′ 3′-(TG_3)$_4$CTCT(ACG)$_2$-5′	515/577		39.7				
Gap 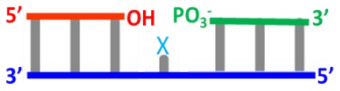	84) 5′-GCTCATG_2TG_2 $G_2CAGCGC_2TC$-3′ 3′-CGAGTAC_2AC_2X$C_2GTCGCG_2AG$-5′ X = A, T, C or G	560/643 (X = C)	N/A	47.2	1:15:3	20 mM PBS with 1 mM Mg^{2+}, pH 7	- Base opposite to gap site is represented as X. - Bright fluorescence only forms when X is C. - Absence of phosphate at gap site gives fast evolution of 1.5 h.	35
	85) 5′-$C_2ACG_2ATCTGA$ $G_3TGA_3TAT_2CTC$-3′ 3′-$G_2TGC_2TAGACT$X$C_3ACT_3ATA_2GAG$-5′ X = A, T, C or G	585/665 (X = C)						
AP site 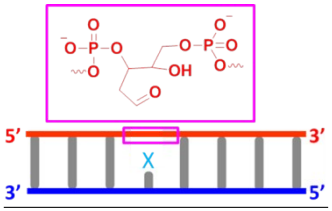	**Y** = AP site; X = A, T, C or G						- Flanking bases are shown in red. - Base opposite to AP site is represented as X.	

	DNA sequence	$\lambda_{ex}/\lambda_{em}$ (nm)	N_{Ag}	Quantum Yield (%)	Synthesis ratio (DNA:Ag^+:BH_4^-)	Buffer	Remarks	Ref.
(i) Flanking Bases & the base opposite to AP site:	86) 5′-ATG$_2$TGGYGGCAGCG-3′ 3′-TAC$_2$ACCXCCGTCGC-5′	588/670 (X = C)	N/A	N/A	1:10:11.6	20 mM PBS, 1 mM $Mg(OAc)_2$, pH 7	- Only forms bright fluorescence when X is C. - Both flanking bases must be G.	36
(ii) Number of AP sites:	87) 5′-ATGT$_2$GGYGGTCAGGYGGT$_2$ATG-3′ 3′-TACA$_2$CCCCCAGTCCCCCA$_2$TAC-5′	588/670	2	N/A	DNA/Ag^+ varied; Ag^+:BH_4^- = 4:1	20 mM PBS with 1 mM Mg^{2+}, pH 7	- AgNCs form at AP site. - (87) with two distinct AP sites give higher emission intensity than that with one AP site. - Two consecutive AP sites in (88) results in blue shift of λ_{em} and larger AgNCs.	37
	88) 5′-ATG$_2$TGGYYGGCAGCG-3′ 3′-TAC$_2$ACCCCCCGTCGC-5′	550/618	4					
(iii) Sequences one base away from AP site:	89) 5′-ATG$_2$TMGYGPCAGCG-3′ 3′-TAC$_2$ANCCCQGTCGC-5′ M/P = A, T, C or G; N/Q = complement to M/P	468–585/546–667 (refer to 'Remarks')	2	N/A	DNA/Ag^+ varied; Ag^+:BH_4^- = 4:1	20 mM PBS with 1 mM Mg^{2+}, pH 7	- N_{Ag} is determined from Job's plot of emission intensity *vs.* [DNA]:[Ag^+]. - When M = G and P is varied; λ_{em} red-shifts from 546 to 670 nm, in the order of T < C < A < G. - When P = G and M is varied; λ_{em} red shifts from 619 to 670 nm, in the order of T < C < A < G.	37
Mismatched site 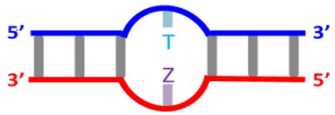							- Mismatched base pairs are in blue and purple.	
(i) Mismatched site with T:	90) 5′-C$_3$TA$_2$C$_3$TA$_2$C$_3$TA$_2$C$_3$T-3′ 3′-G$_3$AT$_2$G$_3$ZT$_2$G$_3$AT$_2$G$_3$A-5′ Z = A, T, C or G;	520/570 (Z = T)	3–6 (Z = T)	8.1 %	1:6.6:6.6	10 mM Tris-HNO_3	- N_{Ag} is determined from ESI-MS. - Fluorescence intensity increases follows the order of T–C > T–G > T–T. - Fluorescence intensity increases as number of T–T mismatched increases.	38
	91) 5′-G$_2$CACA$_3$CACGCAC$_2$TCA$_2$-3′ 3′-C$_2$GTGT$_3$GTTCGTG$_2$AGT$_2$-5′	520/570	N/A	N/A				
	92) 5′-AG$_3$T$_2$TG$_3$T$_2$AG$_3$T$_2$TG$_3$-3′ 3′-TC$_3$A$_2$TC$_3$A$_2$TC$_3$A$_2$TC$_3$-5′	520/570						
(ii) Mismatched site with C:	93) 5′-GCATGTAC$_2$C$_n$G$_2$A$_2$GATCG-3′ 3′-CGTACATG$_2$C$_n$C$_2$T$_2$CTAGC-5′	563/654 (n = 4)	4 (n = 4)	N/A	1:4:2	20 mM PBS with 1 mM	- N_{Ag} is determined from Job's plot of emission	39

	DNA sequence	$\lambda_{ex}/\lambda_{em}$ (nm)	N_{Ag}	Quantum Yield (%)	Synthesis ratio ($DNA:Ag^+:BH_4^-$)	Buffer	Remarks	Ref.
	n = 3, 4, 5					Mg^{2+}, pH 7	intensity *vs.* [DNA]:[Ag^+]. - One-size AgNCs form when n = 4; whereas n = 3 & 5 shows large wavelength-dependent emission ($\Delta\lambda_{em}$ = 150 nm). - Presence of low concentration of halides can enhance the fluorescence.	
Bulge 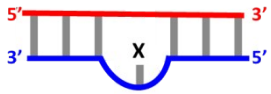 (i) Bulge C:	**X** = bulge base (A, T, C or G) 94) 5'-ATG$_2$TGG GGCAGCG-3' 3'-TAC$_2$AC**X**CCGTCGC-5'	589/652 (**X** = C)	N/A	N/A	1:15:6	PBS with 1 mM Mg^{2+}, pH 7	- Flanking bases are shown in red and blue. - Only **X** = C gives bright fluorescence. The bulge site has to be surrounded by context G. - (94)-AgNCs are 6.7x and 2x brighter than the corresponding gap- and AP-derived AgNCs.	40
(ii) Bulge T:	95) 5'-CGCTGCG**X**GCAC$_2$AT-3' 3'-GCGACGC CGTG$_2$TA-5'	565/624 (**X** = T)	N/A	N/A	1:15:6	20 mM PBS with 1 mM Mg^{2+}, pH 7	- Only **X** = T gives bright fluorescence, presumably bulge T located in a more intrahelical state which allows better Ag^+-binding. - Stacking interaction with flanking bases may also affect the electronic properties of AgNCs.	41
Loop 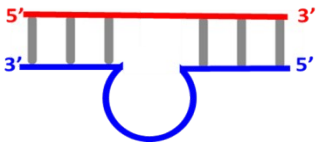 (i) Effect of loop size and distance of mutation point:	5'-GTGCAC$_2$TGACTC$_2$TGTG$_2$AGA$_2$G-3' 3'-CACGTG$_2$ACTGAG$_2$–C$_n$– CAC$_2$TCT$_2$C-5'						- Mutation points are shown in red. - Mutation point should be < 3 bases away from loop. Only fully matched duplex	42

	DNA sequence	$\lambda_{ex}/\lambda_{em}$ (nm)	N_{Ag}	Quantum Yield (%)	Synthesis ratio (DNA:Ag^+:BH_4^-)	Buffer	Remarks	Ref.
	96) n = 4	485/560; 560/630	N/A	N/A	1:6:6	20 mM PBS, 1 mM $Mg(OAc)_2$, pH 7	forms bright fluorescence. - n = 6 gives the best differentiation between fully matched and mismatched stem region.	
	97) n = 6	520/572		34 ± 2				
	98) n = 8	560/620		N/A				
(ii) Identity of mutation point:	99) 5'-$G_2AT_2AT_2GT_2A_3TAT_2GATA_2G_2ATATA$-3' 3'-$C_2TA_2TA_2CA_2T_2$ –C_6– $TATA_2CTAT_2C_2TATAT$-5'	476/545	N/A	N/A	1:6:6	20 mM PBS, 1 mM $Mg(OAc)_2$, pH 7	- Matched T/A gives the most distinctive signal than other mutation points. Other matched base pairs are distinguishable from their mutated analogues but with much weaker signal.	42
(iii) Strand exchange reaction:	100) 5'-CT_2CTC_2A –C_6– $CAG_2AGTCAG_2TGCAC$-3' (S1) 3'- $GA_2GAG_2AGTC_2TCAGTC_2ACGTGACT_2GAT_2$ GT-5' (S2)	575/635	N/A	N/A	1:6:6	20 mM PBS, 1 mM $Mg(OAc)_2$, pH 7	- S1 and S2 are complementary (except extra sequences in S2 highlighted in orange) - Adding another strand wholly complement to S2 can disrupt the hybridization and turn off the fluorescence.	43

Table S5. A summary on design of NCB

	DNA sequence [a]	$\lambda_{ex}/\lambda_{em}$ (nm)	Enhancement ratio	Synthesis ratio (DNA: Ag^+: BH_4^-)	Buffer	Remarks	Ref.
Polytcytosine heads (C_{n1} and C_{n2}):	101) C_2TTAATC_2	580/650	1851 ± 686	1:12:6	20 mM PBS, pH6.7	- Longer C_n gives higher emission intensity. - Emission peak blue-shifts as the length (n) increases.	44
	102) C_3TTAATC_3	645/695	213 ± 8				
	103) C_3TTAATC_4	580/640	3465 ± 928				
	104) C_4TTAATC_4	580/635	760 ± 97				
	105) C_5TTAATC_5	525/585	408 ± 6				
	106) C_6TTAATC_6	525/590	242 ± 6				
	107) C_7TTAATC_7	525/590	62 ± 13				
	108) C_8TTAATC_8	460/555	24 ± 2				
Linker (NNNNN):	109) C_3TC_4	649 [b]	356 ± 15	1:12:6	20 mM PBS, pH6.7	- Adding T to 3' side of linker causes red shift. - Adding A to 3' side of linker cause blue shift. - Placing C (underlined) close to polyC heads tends to activate green-emitting species.	44
	110) C_3TTC_4	646 [b]	479 ± 28				
	111) C_3TTAC_4	646 [b]	324 ± 7				
	112) C_3TTAAC_4	633 [b]	824 ± 105				
	113) C_3TTAATC_4	636 [b]	3465 ± 928				
	114) C_3TTAATTC_4	650 [b]	238 ± 17				
	115) C_3TTAATTAC_4	635 [b]	659 ± 87				
	116) C_3TTAATTAAC_4	632 [b]	527 ± 73				
	117) C_3TTAATTAATC_4	637 [b]	398 ± 17				
	118) C_3TTAATTAATTC_4	655 [b]	219 ± 11				
	119) C_3CTAATC_4	640 [b]	161 ± 9				
	120) C_3TCAATC_4	630 [b]	413 ± 79				
	121) C_3TTCATC_4	640 [b]	579 ± 27				
	122) C_3TTACTC_4	620 [b]	132 ± 5				
	123) C_3TTAACC_4	635 [b]	277 ± 18				
Enhancer (hanging region):	124) T_{12}	490/535	N/A	1:6:6	20 mM PBS, pH 6.6	- PolyG tends to stabilise red-emitting species. - PolyT tends to stabilise green-emitting species.	45,46
	125) $G_3(AG_4)_3$	520/590	N/A				
	126) $G_3(TG_4)_3$	580/636	N/A				

[a] Sequence of the relevant component. Full sequence is not shown at here.

[b] λ_{em}

Table S6. Selected tsDNA templates used to form AgNCs

	DNA sequence	$\lambda_{ex}/\lambda_{em}$ (nm)	N_{Ag}	Quantum Yield (%)	Synthesis ratio ($DNA:Ag^+:BH_4^-$)	Buffer	Remarks	Ref.
tsDNA 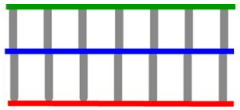	127) 5′-TCTCTCTCTCTCTT-3′ 3′-AAGAGAGAGAGAGGA-5′ 5′-TTCTCTCTCTCTCT-3′	N/A	N/A	N/A	1:6:24 or 1:8:32	10 mM PBS, containing 100 mM $NaNO_3$	- N_{Ag} is determined from ESI-MS. - CG·C⁺ sites are shown in red. - (128)-AgNCs with two successive CG·C⁺ sites give the best result; (129)-AgNCs with three successive sites form multiple species. - Emission intensity increases as number of CG·C⁺ sites increases (*i.e.* (131)-AgNCs give higher intensity than (130)-AgNCs).	47
	128) 5′-TTCCTTCCTTCCTT-3′ 3′-AAGGAAGGAAGGAA-5′ 5′-TTCCTTCCTTCCTT-3′	480/534	2					
	129) 5′-TTCCCTTTTCCCTT-3′ 3′-AAGGGAAAAGGGAA-5′ 5′-TTCCCTTTTCCCTT-3′	420–480/ 530–550	3					
	130) 5′-TTCCTTTTTTCCTT-3′ 3′-AAGGAAAAAAGGAA-5′ 5′-TTCCTTTTTTCCTT-3′	480/534	N/A					
	131) 5′-TTCCTTCCTTCCTTCCTT-3′ 3′-AAGGAAGGAAGGAAGGAA-5′ 5′-TTCCTTCCTTCCTTCCTT -3′	480/534	N/A					
X-shaped DNA 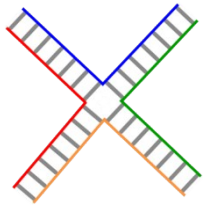	132) 5′-CGA CCG ATG AAT AGC GGT CAG ATC CGT ACC TAC TCG-3′ 5′-CGA GTA GGT ACG GAT CTG CGT ATT GCG AAC GAC TCG -3′ 5′-CGA GAC CAT ACG TAG AGC ACC GCT ATT CAT CGG TCG -3′ 5′-CGA GTC GTT CGC AAT ACG GCT GTA CGT ATG GTC TCG -3′	520/621	N/A	19.8	1:7:14	50 mM NH_4OAc	- (132) and (133) contains composition ratio of C & G of 55.6%. - (132)-AgNCs show brighter fluorescence as it contains one additional arm. - (133)-AgNCs show slower reaction which may due to smaller number of base-pairs.	48
Y-shaped DNA 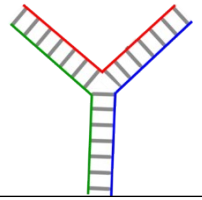	133) 5′-CGA CCG ATG AAT AGC GGT CAG ATC CGT ACC TAC TCG -3′ 5′-CGA GTC GTT CGC AAT ACG ACC GCT ATT CAT CGG TCG -3′ 5′-CGA GTA GGT ACG GAT CTG CGT ATT GCG AAC GAC TCG-3′	N/A/630	N/A	11.1	1:7:14	50 mM NH_4OAc		48

References:

1. J. T. Petty, J. Zheng, N. V. Hud, R. M. Dickson, *J. Am. Chem. Soc.*, 2004, **126**(16), 5207.
2. D. Schultz, E. Gwinn, *Chem. Commun*., 2011, **47**(16), 4715.
3. C. M. Ritchie, K. R. Johnsen, J. R. Kiser, Y. Antoku, R. M. Dickson, J. T. Petty, *J. Phys. Chem.* C., 2007, **111**(1),175.
4. T. Vosch, Y. Antoku, J. Hsiang, C. I. Richards, J. I. Gonzalez, R. M. Dickson, *Proc. Natl. Acad. Sci. U.S.A.*, 2007, **104**(31), 12616.
5. Y. Antoku, Fluorescent Polycytosine-Encapsulated Silver Nanoclusters, Georgia Institute of Technology, 2007.
6. B. Sengupta, C. M. Ritchie, J. G. Buckman, K. R. Johnsen, P. M. Goodwin, J. T. Petty, *J. Phys. Chem. C.*, 2008, **112**, 18776.
7. H. Liu, Y. Wang, L. Zhang, Y. Shao, B. Zheng, *Mater. Lett.*, 2015, **139**, 265.
8. G. Y. Lan, W. Y. Chen, H. T. Chang, *RSC Adv*., 2011, **1**(5), 802.
9. C. I. Richards, S. Choi, J. C. Hsiang, Y. Antoku, T. Vosch, A. Bongiorno, Y. L. Tzeng, R. M. Dickson. *J. Am. Chem. Soc.*, 2008, **130**(15), 5038.
10. Z. Huang, J. Ren, W. Yang, X. Qu, *Chem. Commun.*, 2013, **49**(92), 10856.
11. J. Sharma, H. C. Yeh, H. Yoo, J. H. Werner, J. S. Martinez, *Chem. Commun.*, 2010, **46**(19), 3280.
12. M. L. Neidig, J. Sharma, H. C. Yeh, J. S. Martinez, S. D. Conradson, A. P. Shreve, *J. Am. Chem. Soc.*, 2011, **133**, 11837.
13. G. Liu, D. Q. Feng, X. Mu, W. Zheng, T. Chen, L. Qi, D. Li, J. *Mater. Chem. B.*, 2013, **1**(16), 2128.
14. D. Schultz, E. G. Gwinn, *Chem. Commun.* 2012, **48**(46), 5748.
15. J. T. Petty, C. Fan, S. P. Story, B. Sengupta, A. S. J. Iyer, Z. Prudowsky, R, M. Dickson, *J. Phys. Chem. Lett.*, 2010, **1**(17), 2524.
16. J. T. Petty, C. Fan, S. P. Story, B. Sengupta, M. Sartin, J. C. Hsiang, J. W. Perry, R. M Dickson, *J. Phys. Chem. B.*, 2011, **115**(24), 7996.
17. J. Sharma, R. C. Rocha, M. L. Phipps, H. C. Yeh, K. A. Balatsky, D. M. Vu, A. P. Shreve, J. H. Werner, J. S. Martinez, *Nanoscale*, 2012, **4**(14), 4107.
18. J. L. Ma, B. C. Yin, B. C. Ye, *RSC Adv.*, 2015, **5**(119), 98467.
19. J. T. Petty, B. Giri, I. C. Miller, D. A. Nicholson, O. O. Sergev. T. M. Banks, S. P. Story, *Anal. Chem.*, 2013, **85**, 2183.
20. J. T. Petty, O. O. Sergev, A. G. Kantor, I. J. Rankine, M. Ganguly, F. D. David, S. K. Wheeler, J. F. Wheeler, *Anal. Chem.*, 2015, **87**(10), 5302.
21. D. Schultz, K. Gardner, S. S. R. Oemrawsingh, N. Markešević, K. Olsson, M. Debord, D. Bouwmeester, E. Gwinn, *Adv. Mater.*, 2013, **25**(20), 2797.
22. B. Sengupta, K. Springer, J. G. Buckman, S. P. Story, O. H. Abe, Z. W. Hasan, Z. D. Prudowsky, S. E. Rudisill, N. N. Degtyareva, J. T. Petty, *J. Phys. Chem. C.*, 2009, **113**, 19518.
23. W. Li, L. Liu, Y. Fu, Y. Sun, J. Zhang, R. Zhang, *Photochem. Photobiol. Sci.*, 2013, **12**(10), 1864.
24. T. Li, N. He, J. Wang, S. Li, Y. Deng, Z. Wang, *RSC Adv.*, 2016, **6**(27), 22839.
25. J. Ai, W. Guo, B. Li, T. Li, D. Li, E. Wang, *Talanta*, 2012, **88**, 450.
26. H. C. Hsu, M. C. Ho, K. H. Wang, Y. F. Hsu, C. W. Chang, *New J. Chem.*, 2015, **39**(3), 2140.
27. T. Li, L. Zhang, J. Ai, S. Dong, E. Wang, *ACS Nano.*, 2011, **5**(8), 6334.
28. P. R. O'Neill, K. Young, D. Schiffels, D. K. Fygenson, *Nano Lett.*, 2012, **12,** 5464.
29. P. R. O'Neill, L. R. Velazquez, D. G. Dunn, E. G. Gwinn, D. K. Fygenson, *J. Phys. Chem. C.*, 2009, **113**, 4229.
30. E. G. Gwinn, P. R. O'Neill, A. J. Guerrero, D. Bouwmeester, D. K. Fygenson, *Adv. Mater.*, 2008, **20**(2), 279.
31. J. Li, X. Jia, D. Li, J. Ren, Y. Han, Y. Xia, E. Wang, *Nanoscale*, 2013, **5**(13), 6131.
32. I. Tinoco, O. C. Uhlenbeck, M. D. Levine, *Nature*, 1971, **230**, 362.
33. K. Morishita, J. L. MacLean, B. Liu, H. Jiang, J. Liu, *Nanoscale*, 2013, **5**(7), 2840.
34. J. Zhu, L. Zhang, Y. Teng, B. Lou, X. Jia, X. Gu, E. Wang, *Nanoscale*, 2015, **7**(31), 13224.
35. Q. Cui, K. Ma, Y. Shao, S. Xu, F. Wu, G. Liu, N. Teramae, H. Bao, *Anal. Chim. Acta.*, 2012, **724**, 86.
36. K. Ma, Q. Cui, G. Liu, F. Wu, S. Xu, Y. Shao, *Nanotechnology.*, 2011, **22**(30), 305502.
37. K. Ma, Y. Shao, Q. Cui, F. Wu, S. Xu, G. Liu, *Langmuir*, 2012, **28**, 15313.
38. Z. Huang, F. Pu, D. Hu, C. Wang, J. Ren, X. Qu, *Chem. Eur. J.*, 2011, **17**(13), 3774.
39. J. Peng, Y. Shao, L. Liu, L. Zhang, W. Fu, H. Liu, *Nanotechnology*, 2014, **25**(23), 235501.
40. J. Peng, Y. Shao, L. Liu, L. Zhang, H. Liu, *Dalt. Trans.*, 2014, **43**(4), 1534.
41. J. Peng, Y. Shao, L. Liu, L. Zhang, H. Liu, Y. Wang, *Anal. Chim. Acta.*, 2014, **850**, 78.
42. W. Guo, J. Yuan, Q. Dong, E. Wang. *J. Am. Chem. Soc.*, 2010, **132**, 932.
43. W. Guo, J. Yuan, E. Wang, *Chem. Commun.*, 2011, **47**(39), 10930.
44. J. M. Obliosca, M. C. Babin, C. Liu, Y. Liu, Y. Chen, R. A. Batson, M. Ganguly, J. T. Petty, H.C. Yeh, *ACS Nano.*, 2014, **8**(10), 10150.
45. H. C. Yeh, J. Sharma, J. J. Han, J. S. Martinez, J. H. Werner, *Nano Lett.*, 2010, **1**, 3106.
46. H. C. Yeh, J. Sharma, J. J. Han, J. S. Martinez, J. H. Werner, *IEEE Nanotechnol. Mag.*, 2011, p. 28.
47. L. Feng, Z. Huang, J. Ren, X. Qu, *Nucleic Acids Res.*, 2012, **40**(16), 1.
48. J. Park, J. Song, J. Park, N. Park, S. Kim, *Bull. Korean Chem. Soc.*, 2014, **35**(4), 1105.